Bile Salt Aggregates in the Gas Phase: An Electrospray Ionization Mass Spectrometric Study

Fulvio Cacace,*[a] Giulia de Petris,[a] Edoardo Giglio,*[b] Francesco Punzo,[b] and Anna Troiani[a]

Abstract: Helical and ordered structures have previously been identified by X-ray diffraction analysis in crystals and fibers of bile salts, and proposed as models of the micellar aggregates formed by trimeric or dimeric units of dihydroxy and trihydroxy salts, respectively. These models were supported by the results of studies of micellar bile salt solutions performed with different experimental techniques. The study has now been extended to the gas phase by utilizing electrospray ionization mass spectrometry (ESIMS) to investigate the formation and the composition of aggregates stabilized by noncovalent interactions, including polar (ion–ion, ion–dipole, dipole–dipole, hydrogen bonding etc.) and apolar (van der Waals and repulsive) interactions. The positive and negative ESIMS spectra of sodium glycodeoxycholate (NaGDC), taurodeoxycholate (NaTDC), glycocholate (NaGC), and taurocholate (NaTC) aqueous solutions, recorded under different experimental conditions, show in the first place that aggregates analogous to those present in micellar solutions do also exist in the gas phase. Furthermore, consistently with the condensed-phase model, the positive-ion spectra show that the trimers are the most stable oligomers among the aggregates of dihydroxy salts (NaGDC and NaTDC) whilst the dimers are the most stable among the aggregates of trihydroxy salts (NaGC and NaTC). Moreover, the binding energy of the constituent glycocholate salt units in most gaseous oligomers exceeds that of the corresponding taurocholate units. The ESIMS evidence has been confirmed by vapor-pressure measurements performed on NaGC and NaTC crystals and NaGDC and NaTDC fibers, the results of which show that the evaporation enthalpy of glycocholate exceeds that of taurocholate by some 50 kJ mol^{-1}.

Keywords: bile salts · gas-phase reactions · mass spectrometry · micelles · noncovalent interactions

Introduction

Bile salts are natural steroids, showing surface-active and detergent-like properties, capable of forming micellar aggregates in aqueous solutions.[1–4] They can interact with and solubilize many compounds, such as cholesterol, fatty acids, bilirubin-IXα, phospholipids, and proteins, that play a pivotal role in biological systems. Moreover, considerable attention has recently been focused on the metabolic significance of bile salts in hepatobiliary diseases. Knowledge of the structure and composition of the bile salt micellar aggregates is crucial for comprehending their physicochemical and biomedical properties, but it remains a *vexata quaestio*, as witnessed by the widely different models proposed.[5–9]

Bile salt anions have one relatively rigid moiety (three cyclohexane and one cyclopentane rings) and one flexible one (the side chain ending with a carboxylate or sulfonate group). They present an arched shape due to the *cis* fusion of two cyclohexane rings (A and B), and are two-faced, showing a polar face (α, characterized by hydroxy groups) and an apolar one (β, characterized by the C_{18} and C_{19} methyl groups). Bile salts have hydroxy functions at positions 3α and 12α (dihydroxy salts) or at 3α, 7α, and 12α (trihydroxy salts). Those relevant to this study (Figure 1) are the sodium salts of 3α,12α-dihydroxy-5β-cholanoyltaurine (sodium taurodeoxycholate, NaTDC), 3α,12α-dihydroxy-5β-cholanoylglycine (sodium glycodeoxycholate, NaGDC), 3α,7α,12α-trihydroxy-5β-cholanoyltaurine (sodium taurocholate, NaTC), and 3α,7α,12α-trihydroxy-5β-cholanoylglycine (sodium glycocholate, NaGC).

Although dihydroxy and trihydroxy bile salts show highly dissimilar physicochemical properties,[4] and hence their micellar aggregates are highly unlikely to possess similar structures, aggregation models with a poorly defined packing

[a] Prof. Dr. F. Cacace, Prof. Dr. G. de Petris, Dr. A. Troiani
Dipartimento di Studi di Chimica e Tecnologia
delle Sostanze Biologicamente Attive
Università di Roma "La Sapienza"
P.le Aldo Moro 5, 00185 Roma (Italy)
Fax: (+390) 6-49913602
E-mail: fulvio.cacace@uniroma1.it

[b] Prof. Dr. E. Giglio, Dr. F. Punzo
Dipartimento di Chimica
Università di Roma "La Sapienza"
P.le Aldo Moro 5, 00185 Roma (Italy)
Fax: (+390) 6-490631
E-mail: e.giglio@caspur.it

  0947-6539/02/0808-1925 $ 20.00+.50/0

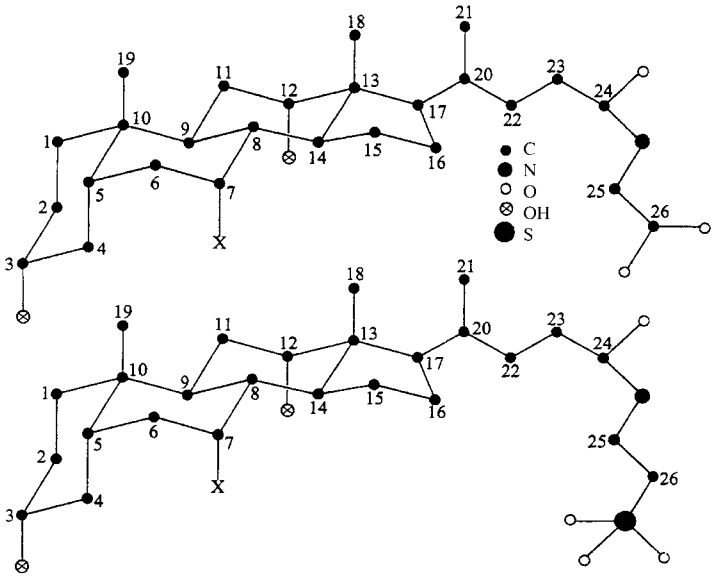

Figure 1. Carbon atoms numbering of bile salt anions relevant to this work. Hydrogen atoms are omitted for the sake of clarity. From top to bottom: X = H, taurodeoxycholate, and glycodeoxycholate; X = OH, taurocholate, and glycocholate.

structure and valid for all dihydroxy and trihydroxy bile salts have been proposed. Among others, that of Small[5] and, to a lesser extent, those of Oakenfull and Fisher[6] and Kawamura et al.[7] have frequently been used to interpret experimental data. Small[5] assumed that small numbers of bile salt molecules aggregate by means of hydrophobic interactions, giving rise to primary micelles. At higher concentrations, the primary micelles form larger secondary micelles by polymerization in a linear fashion through hydrogen bonding. Oakenfull and Fisher[6] suggested dimer formation through hydrogen bonds. Kawamura et al.[7] proposed a disklike structure in which bile salt anions have their long molecular axes parallel, or approximately parallel (probably 50% pointing up and 50% pointing down). Because of some discrepancies that arise from these and other models and cast doubt on their reliability, a study on bile salts and their interaction complexes with selected probe molecules was undertaken. This was done with a variety of experimental techniques both commonly used and less conventional in the micelle field, including measurements of small-angle X-ray scattering, electron spin[10] and nuclear magnetic resonance,[11] quasielastic light scattering,[9a–c, 12] electrolytic conductance,[9c, e] extended X-ray absorption fine structure,[13] electromotive force (EMF),[9a, d, f–i] circular dichroism,[11d, 12a–e, g, 14] X-ray diffraction of crystals and fibers,[9a–e, 12a–c, e, f, 14a, 15] and dielectric spectroscopy.[9c, 12g] The [aqueous micellar solution] → [gel] → [fiber] and, sometimes, the [fiber] → [crystal] transitions are observed for some bile salts. Glassy and birefringent fibers can be drawn from gels or aqueous micellar solutions near the gelation point, and crystals can sometimes be obtained from fibers by aging. Reasonably, the same structural unit, or a very similar one, could be present both in the solid (fiber and crystal) and in the liquid (aqueous micellar solution) state, as frequently occurs for macromolecules. Accordingly, the structures observed in crystals and fibers were used as models that were verified in aqueous micellar solutions. Of course, fiber models are more reliable than crystal ones, because the fiber is a system more similar than the crystal to the aqueous micellar solution. On the other hand, it is probable that [aqueous micellar solution] → [gel] → [fiber] transitions occur without drastic structural changes, since the gel is obtained by concentrating the aqueous micellar solution, and the fiber is drawn from the gel by means of the gentle pull of gravity. Models with well-established packing structures, which aptly represent those of micellar aggregates, have been obtained by resolving several crystal and fiber structures. Fibers of lithium, sodium, potassium, and rubidium deoxycholate[9b, c] or NaTDC, NaGDC, rubidium taurodeoxycholate and glycodeoxycholate,[9a] and calcium taurodeoxycholate[12e] (dihydroxy salts), showed the presence of 8/1 or 7/1 helices, respectively. The basic building block and repetitive unit of both types of helix is a trimer with a threefold rotation axis (Figure 2). These helices satisfactorily represent the micellar aggregate structures. Dimers and octamers of the type found both in NaTC[9d, 12b] and in NaGC[9, 15d] crystals and fibers (see Figure 3 for a NaTC dimer and Figure 4 for a NaGC octamer) suitably represent the building blocks of NaTC and NaGC micellar aggregates (trihydroxy salts). In particular, dimers have a twofold rotation or a twofold screw axis and are arranged in structural units obtained by translation along the dimer

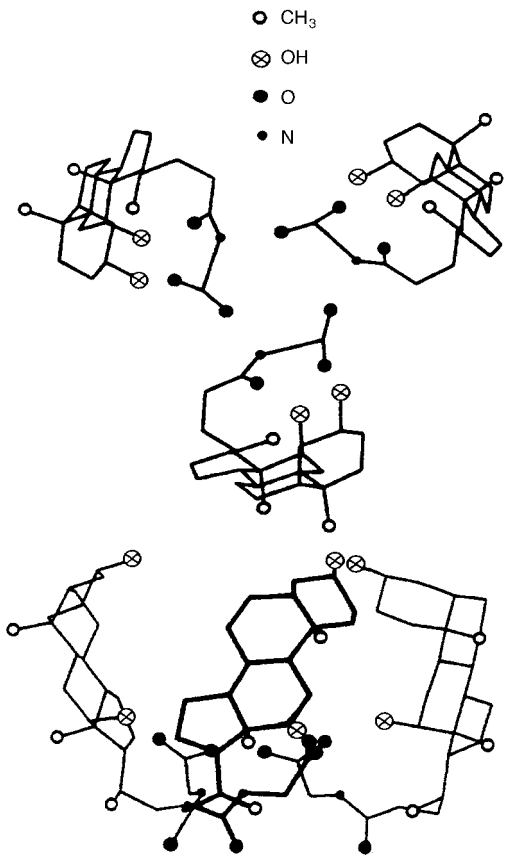

Figure 2. Glycodeoxycholate anion trimer (7/1 helix) projected along the helical axis (top) and an axis perpendicular to the helical axis (bottom). The thicker line represents an anion nearer to the observer.

0947-6539/02/0808-1926 $ 20.00+.50/0 *Chem. Eur. J.* **2002**, *8*, No. 8

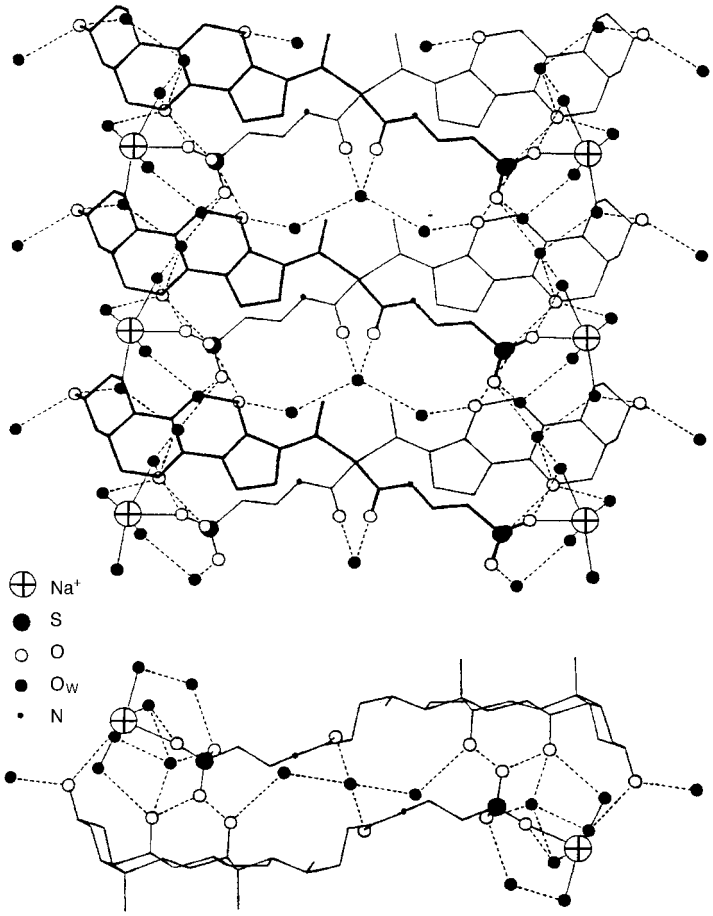

Figure 3. NaTC structural unit with a twofold rotation axis projected along a direction perpendicular to the twofold rotation axis (top) and along the twofold rotation axis (bottom). A thicker line represents an anion nearer to the observer. Broken or thin full lines indicate hydrogen bonds or ion–ion and ion–dipole interactions.

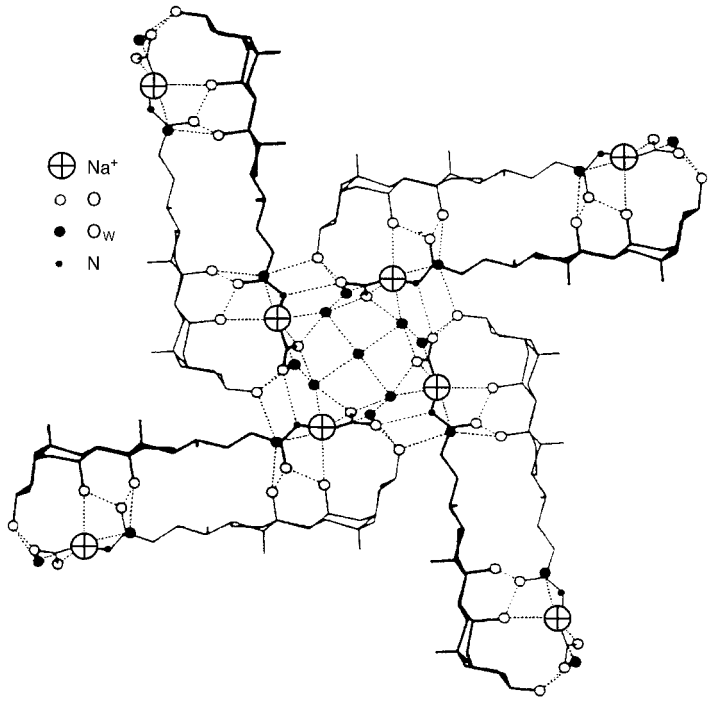

Figure 4. NaGC octamer. Thicker lines represent an anion nearer to the observer. Broken lines indicate ion–ion or ion–dipole interactions or hydrogen bonds.

twofold rotation or screw axis. All the dihydroxy and trihydroxy salt aggregates (including dimers, trimers, and octamers) are stabilized mainly by strong polar interactions, that particularly involve the cations, as inferred from X-ray analysis, electrolytic conductance, and dielectric measurements.[9e] In agreement with the above models, the NaTDC micellar aggregation numbers, obtained from EMF measurements as a function of the ionic strength, pH, and bile salt concentration, are generally multiples of three,[9a, h] whereas NaGDC always shows the presence of trimers, even at the highest ionic strengths.[9g] The aggregation numbers of NaTC[9d, i] and NaGC[9e, 16] micelles are always multiples of two and, when the micellar size increases, are mainly multiples of eight. However, it must be stressed that dimer structural units are also observed in dihydroxy salt crystals,[12a, f] thus supporting the view that this type of structural pattern is a very stable one.

Since, in the liquid phase, the problem is considerably complicated by the influence of environmental factors, a promising approach to the evaluation of the intrinsic structural features of bile salt aggregates is the extension of the study to the gas phase, in which the effects of the medium are minimized. Here we report the first gas-phase investigation of the formation and the composition of gaseous, noncovalent micellar aggregates of bile salts, characterized by polar (ion–ion, ion–dipole, dipole–dipole, hydrogen bonding etc.) and apolar (van der Waals and repulsive) interactions. Our approach is based on electrospray ionization mass spectrometry (ESIMS), a "soft" ionization technique, the successful application of which to other self-organizing systems (proteins, for example) important from a biological and/or a technological standpoint, is well documented.[17] It should be emphasized that in this study the ESIMS experiments have *not* been utilized to gather additional information on the micellar aggregates solution, which is already well characterized by the techniques cited above. Furthermore, bile salt aggregate sizes, structures, and physical and thermodynamic properties in aqueous solutions can hardly be expected to be present in the electrospray ionization process, owing to the intrinsic features of the latter. As stated above, the specific aim of this study is rather to ascertain whether the results of ESIMS experiments can provide information on the existence, the aggregation state, and the stability of *bile salt aggregates in the gas phase*. As a matter of fact, this phase is least perturbed by the effect of the environment, and hence its study is useful to obtain the composition and distribution of aggregates that might be related to the micellar aggregates in aqueous solution.

Results and Discussion

ESI spectra in positive-ion detection mode: ESI spectra of 10^{-3} M aqueous NaGC, NaTC, NaGDC, and NaTDC solutions were recorded at ΔNS values ranging from 0 to 260 V and show similar patterns. As a typical example, Figure 5 illustrates the spectra of NaTC solutions recorded in the positive-ion detection mode at high (Figure 5a) and low (Figure 5b) ΔNS values. Henceforth we denote species containing n bile

  0947-6539/02/0808-1927 $ 20.00+.50/0

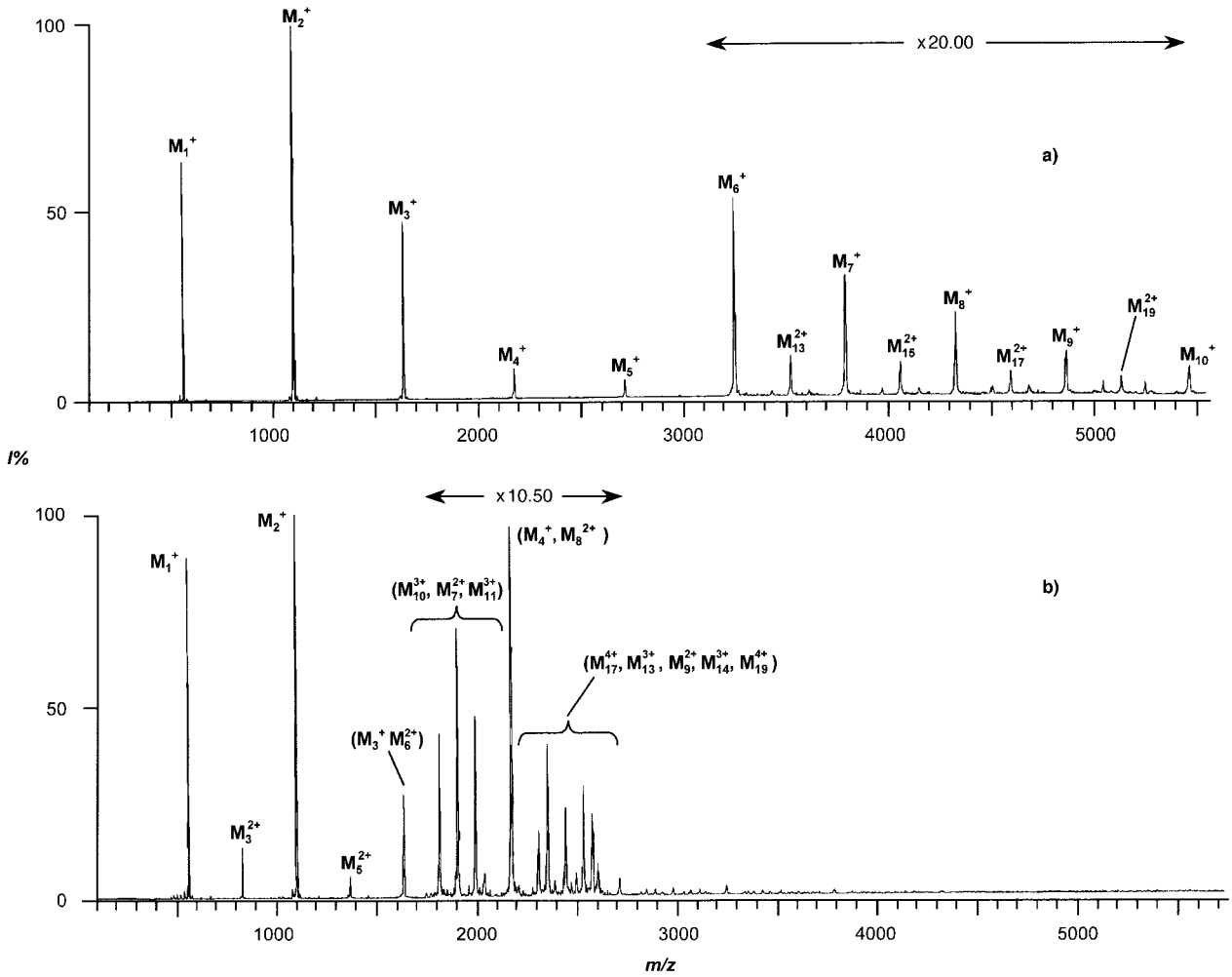

Figure 5. ESI spectra of 10^{-3} M NaTC recorded at $\Delta NS = 260$ V (a) and $\Delta NS = 20$ V (b).

salt molecules and a number b of additional sodium ions as M_n^{b+} (M = one neutral bile salt molecule). It should be noted that, owing to the presence of multicharged ions typical of ESIMS, several ions with different masses and charges that combine to give the same m/z ratio may appear as a single peak. This required performing a charge-state analysis to obtain a correct picture of the ionic population. In the case of interest, the charge-state analysis, from measurement of the $^{12}C/^{13}C$ isotopic peaks separation, demonstrated that, at high ΔNS values (Figure 5a), the first four peaks of the spectrum are indeed singly charged M_n^+ ($n = 1-4$, $b = 1$) ions. A similar positive assignment could not be obtained for peaks at higher m/z ratios, owing to their relatively low intensities. Nevertheless, M_{2n+1}^{2+} ($n = 6-9$, $b = 2$) ions have been detected; these, based on the adopted symbology, denote species containing $2n+1$ salt molecules and two additional sodium ions, giving an indirect hint of the doubly charged M_{2n}^{2+} ion contribution to the $M_6^+ - M_9^+$ peaks (Figure 5a). The presence of doubly charged species at higher n values is in line with the expectation that additional Na^+ ions are more easily accommodated by larger aggregates. At lower ΔNS values (Figure 5b), the charge-state analysis shows that peaks with $n = 1$, 2 are singly charged, whereas the peaks of doubly charged M_6^{2+} and M_8^{2+} ions are superimposed on those of M_3^+ and M_4^+ ions, and this indicates the displacement to lower masses of the multiply charged ion population. This is confirmed by the observation of M_{2n+1}^{2+} ($n = 1-5$) and higher charge-state ($+3$ and $+4$) peaks, as demonstrated by charge-state analysis, performed when allowed by a sufficiently high intensity of the species of interest.

Since dilute solutions of bile salts, such as those utilized in the above experiments, are known mainly to contain monomers and small oligomers,[4, 9a, d, f–i, 12c] one is faced with the question of why larger gaseous aggregates are detected. To clarify this point, a systematic investigation of the ionic population of 10^{-3} M bile salt solutions as a function of the applied ΔNS was performed. The results are illustrated in Figure 6, showing the relative abundances of ten peaks, corresponding to $M_1^+ - M_{10}^+$ ions. The additional dotted line, Mc, shows the combined abundances of all the observed multicharged ions and can be taken as indicative of the extent to which ions of higher charge states, the m/z ratios of which match those of singly charged species, contribute to the population represented by the ten peaks. The Mc line approaches zero at $\Delta NS > 200$ V, confirming that singly charged ions predominate under these conditions, with only a minor contribution from doubly charged species at the highest masses. By contrast, at low ΔNS values, multicharged

0947-6539/02/0808-1928 $ 20.00+.50/0 Chem. Eur. J. 2002, 8, No. 8

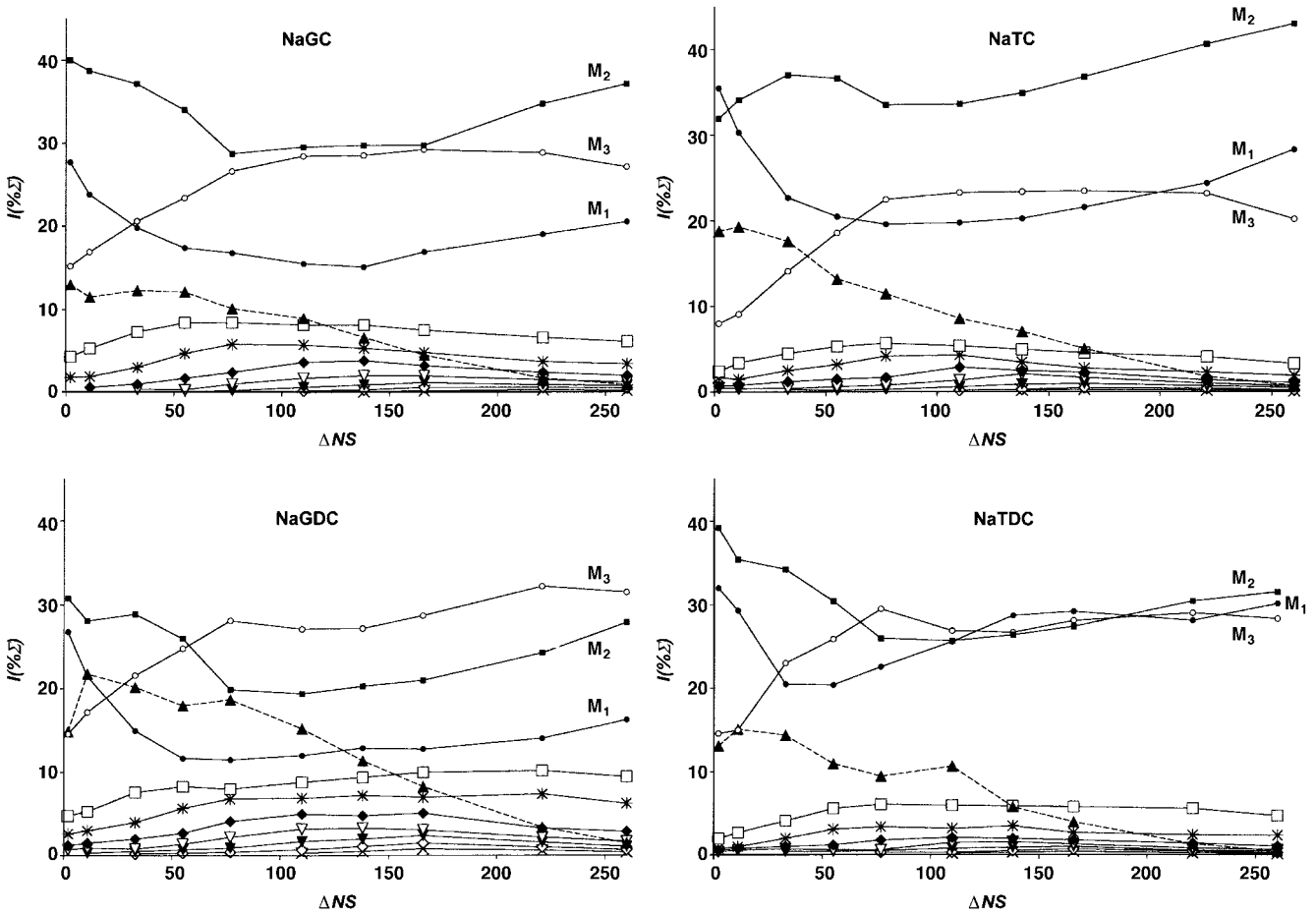

Figure 6. Intensity plots of the M_1-M_{10} positive species of the NaGC, NaTC, NaGDC, and NaTDC ESI spectra as a function of the applied ΔNS (Mc ▲, M_4 □, M_5 *, M_6 ◆, M_7 ▽, M_8 ▼, M_9 ◇, M_{10} ×; M_1, M_2, and M_3 are indicated). The species notation does not indicate the charge state (see text).

species contribute to peaks of lower masses as well. Such a trend raises the question of whether the displacement towards the charge state +1 should be ascribed exclusively to post-source depolymerization processes, more effective at higher ΔNS values and for highly charged ions, or also to a concomitant reduction of the aggregation processes occurring during the spray ionization stage. The question also proves crucial to the assessment of the experimental conditions most representative of the intrinsic features of the system under study in the gas phase. To this end, we recorded ESI spectra of more concentrated (10^{-2} M) aqueous NaTC solutions, at $\Delta NS \cong 0$ V and a 15 μL min^{-1} flow rate, which results in larger droplets, favoring clustering and minimizing desolvation (Figure 7). Charge states ranging from 1 to 9, as well as very large aggregates containing up to 80 salt molecules, were observed. As an example, aggregate charge states within the M_5-M_7 range are reported in the bottom part of Figure 7. The spectrum clearly indicates that ions in higher charge states are to be regarded as the products of aggregation processes, favored by an incomplete charge separation at the higher concentrations momentarily reached in the droplets during the spray process. On the basis of these considerations, ESIMS experiments run at $\Delta NS > 200$ V seem to provide a picture of the populations of the gaseous bile salt aggregates least affected by adventitious processes. Under these conditions, the results show the following.

1) Both NaGC and NaTC display M_2^+ as the most abundant ion.
2) NaGDC displays M_3^+ as the most abundant ion.
3) NaTDC displays comparable abundances of M_1^+, M_2^+, and M_3^+ ions.
4) Higher abundances of peaks with $n > 3$ are shown by NaGC and NaGDC than by NaTC and NaTDC.

Keeping in mind that the initial concentration of the solutions unavoidably increases during the spray process, the composition of the gaseous ion populations from the ESIMS experiments can be used indirectly to support the NaGC, NaTC, NaGDC, and NaTDC structural models proposed for the liquid phase. In this connection, it must be stressed that the gaseous aggregates are dehydrated, so that their structures are different from those existing in aqueous solution. However, crystal structures of almost completely dehydrated bile acid salts are known. As structural units they contain both dimers (rubidium taurocholate[12c] and taurodeoxycholate[12a]) and helices that can easily be traced to an arrangement of trimers (NaTDC[15b] and NaGDC[14a]). Dimer and trimer structures in these crystals are similar to those proposed for the aqueous solution models. Bile acid salt/water ratios are only 1:1 for rubidium taurocholate, rubidium taurodeoxycholate, and NaTDC, and the ratio is 1:1.5 for NaGDC. This strongly suggests that fully dehydrated dimers and trimers structurally similar to those envisaged in the aqueous solution

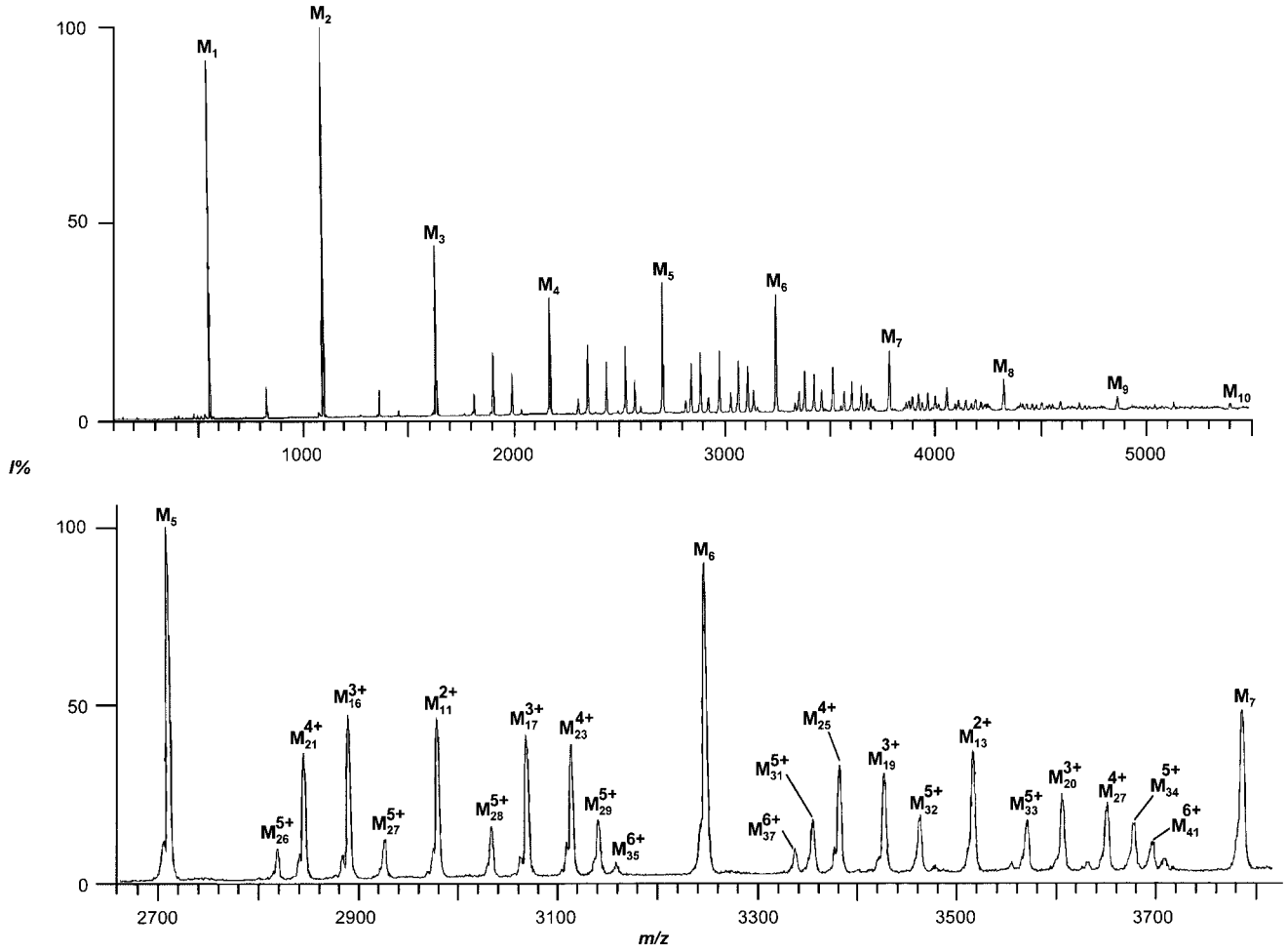

Figure 7. ESI spectrum of 10^{-2} M NaTC recorded at $\Delta NS = 0$ V and a 15 μL min^{-1} flow rate. The $M_1 - M_{10}$ species charge state in the upper part is not specified, owing to the likely superimposition of various charge states. High charge states and high-molecular-weight aggregates within the $M_5 - M_7$ range are shown in the bottom part.

models can be formed in the gas phase. Dimers are the building blocks of NaGC and NaTC micellar aggregates, and trimers those of the NaGDC and NaTDC ones. Thus, the most abundant M_2^+ ions (for NaTC and NaGC), M_3^+ ions (for NaGDC), and M_2^+ and M_3^+ ions (for NaTDC) probably arise from dimers and trimers. Their remarkable abundance in the gas phase, in general greater than that of M_1^+ even under conditions that favor depolymerization (high ΔNS values), suggests that they are particularly stable aggregates. The comparable abundances of M_3^+, M_2^+, and M_1^+ could imply that the NaTDC M_3^+ moiety has a lower stability than the NaGDC one. However, the observation of NaTDC M_2^+ as a major ion is interesting in the light of previous results from the X-ray analysis of a rubidium taurodeoxycholate crystal,[12a] which characterizes the dimer structural pattern as a stable one. The best candidates among the possible structures of M_2^+ and M_3^+ include:

- a dimer with a twofold rotation axis of the type shown in Figure 3, although deprived of water molecules, where two Na^+ ions give rise to the same strong ion–ion and ion–dipole interactions with the sulfonate or the carboxylate group and the hydroxy group at position 3α. A reasonable binding site can also be envisaged for the third Na^+ ion, located near the two carbonylic groups at the center of the dimer, as seen in the projection in Figure 3 (bottom).
- a trimer with a threefold rotation axis of the type shown in Figure 2, in which each pair of carboxylate groups is bridged by one Na^+ ion, and the plane α of the three Na^+ ions is parallel to the least-squares plane β of the three carboxylate groups. A reasonable binding site can be envisaged for the fourth Na^+ ion as well, located on the threefold rotation axis near the carboxylate groups, in the semispace generated by β not containing α.

NaGC and NaGDC give rise to larger abundances of M_n^{b+} ions with $n > 3$ than NaTC and NaTDC do (Figure 6). This behavior can be explained if the glyco derivatives have a higher stability than their tauro derivative counterparts. This is reasonable, since the strongest polar interactions that promote aggregation are those between the Na^+ ions and the polar heads. Because the charge density in CO_2^- is higher than that in SO_3^-, in which the charge is dispersed over a larger volume, the Coulombic interactions of the Na^+ ion with CO_2^- are stronger than with SO_3^-. Supportive experimental evidence is supplied by EMF measurements carried out on NaGC[16] and NaTC[9d, i] as well as on NaGDC[9g] and NaTDC,[9h] because glyco derivative aggregates systematically

  0947-6539/02/0808-1930 $ 20.00+.50/0 *Chem. Eur. J.* **2002**, *8*, No. 8

show association constants larger than those of the corresponding tauro derivatives. However, it must be stressed that the EMF measurements refer to hydrated aggregates. In order to clarify the point, vapor-pressure measurements were performed on NaGC and NaTC crystals, as well as on NaGDC and NaTDC fibers. After the samples had lost water, and also acetone in the cases of NaGC and NaTC, the vaporization enthalpy ΔH°_{T} was evaluated by utilizing equations derived from least-squares treatment of the data relating the vapor pressure of the bile salt monomer P (atm) with the temperature T (K) (standard deviations between brackets, see Eqs. (1) – (4)).

$$\text{NaGC: } \log P = -9837\ (\pm 53)/T + 13.11\ (\pm 0.09); \quad \Delta H^{\circ}_{570} = 188\ (\pm 1)\ \text{kJ mol}^{-1} \quad (1)$$

$$\text{NaTC: } \log P = -7030\ (\pm 161)/T + 7.37\ (\pm 0.27); \quad \Delta H^{\circ}_{600} = 134\ (\pm 3)\ \text{kJ mol}^{-1} \quad (2)$$

$$\text{NaGDC: } \log P = -8994\ (\pm 168)/T + 10.86\ (\pm 0.29); \quad \Delta H^{\circ}_{570} = 172\ (\pm 3)\ \text{kJ mol}^{-1} \quad (3)$$

$$\text{NaTDC: } \log P = -7100\ (\pm 185)/T + 7.21\ (\pm 0.32); \quad \Delta H^{\circ}_{570} = 136\ (\pm 4)\ \text{kJ mol}^{-1} \quad (4)$$

It is very likely that the structures of the molten bile salt small aggregates, in the absence of water, mimic those typical in the gas phase. Moreover, NaGC and NaGDC show ΔH°_{T} values larger by some 40 – 50 kJ mol^{-1} than those of NaTC and NaTDC, consistent with the trends prevailing in ESIMS experiments.

ESI spectra in negative-ion detection mode: The spectra of 10^{-3} M aqueous NaGC, NaTC, NaGDC, and NaTDC solutions were recorded in the ΔNS range from 0 to 260 V. A typical NaTC spectrum, recorded at $\Delta NS = 260$ V, shows the relative abundances of nine peaks, the m/z ratios of which correspond to those of $M_1^- - M_9^-$ ions (Figure 8). It should be noted that M_n^- here, at variance with the notation adopted for positive-ion ESIMS, denotes an aggregate formed by n neutral salt molecules that has been deprived of one Na^+ ion, and this results in the formation of a singly charged anion. The charge-state analysis demonstrated that the first two peaks of the spectrum were indeed singly charged M_n^- ($n = 1, 2$) ions. A similar reliable assignment could not be obtained for peaks of higher m/z ratios, owing to their relatively low intensities.

M_1^- and M_2^- ions are the most abundant species. In contrast with the positive-ion spectra, M_1^- has a relative intensity greater than that of M_2^-. Furthermore, $M_3^- - M_9^-$ ions have relative intensities systematically lower than those of the corresponding $M_3^+ - M_9^+$ ions. The more effective depolymerization processes in the case of negative ions provide strong evidence of their lower stability in comparison with that of the positive ones. As a consequence, and consistently with the experimental results, the formation of multiply charged anions is unlikely, and the ESI spectra are expected to reflect the enhanced rate of depolymerization processes as they displayed low abundances of the higher oligomers. In this connection, it is interesting that, unlike in the cationization process, in which an additional Na^+ ion is unlikely to impair the stability of a gaseous aggregate, the loss of a Na^+ ion is expected to decrease the stability of the M_n^- oligomers significantly. As a general remark, the negative-ion spectra are less structurally informative and less amenable to comparison with the condensed-phase results. As a matter of fact, M_1^- is the most abundant species from NaTC and NaTDC solutions under all experimental conditions, as is also the case with NaGC and NaGDC solutions in the ΔNS range

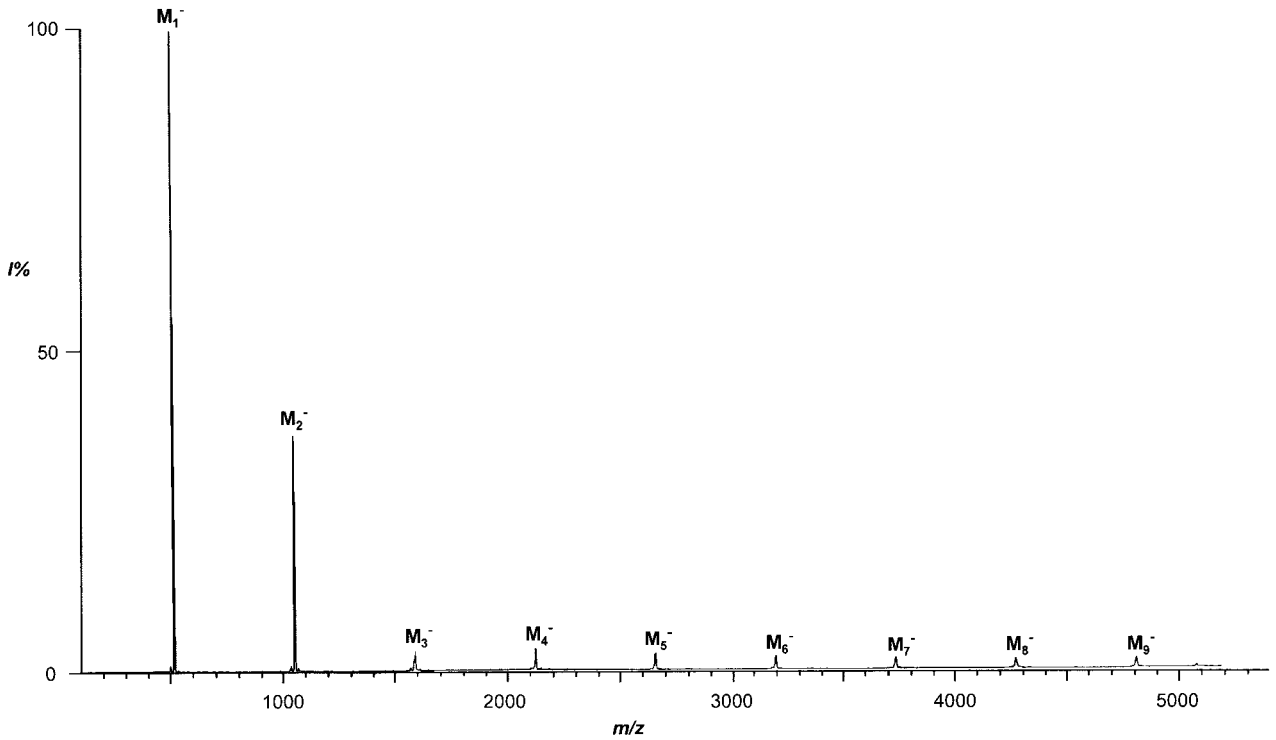

Figure 8. ESI spectrum of a 10^{-3} M NaTC solution in the negative-ion mode, $\Delta NS = 260$ V.

up to ≈100 V, above which the M_2^- anion predominates. Moreover, M_1^- and M_2^- relative abundances show opposite trends, decreasing and increasing, respectively, at higher Δ*NS* values, but in the cases of NaTC and NaTDC, within the range 0 – ≈100 V, their relative abundances are approximately constant. The experimental data can be reasonably explained if M_2^- is a very stable ion, significantly more stable than M_1^-. Indeed, M_2^- is very probably characterized by two carboxylate or sulfonate groups bridged by one Na^+ ion, and this gives rise to strong Coulombic interactions that make its formation energetically favored over that of M_1^-. On the other hand, the high relative abundance of M_1^- reflects its high concentration in the solutions sampled.

Finally, over the entire Δ*NS* range, NaGC and NaGDC display higher abundances of peaks with $n > 2$ than do NaTC and NaTDC. This behavior points to a higher stability of NaGC and NaGDC dimeric anions, probably traceable to the strong polar link between two carboxylate groups and a bridging Na^+ cation. Such stabilizing interactions are weaker in NaTC and NaTDC aggregates, because of the lower charge density of their SO_3^- groups as compared with CO_2^- groups.

Conclusion

The evidence from this ESIMS study firstly shows that noncovalent bile salt aggregates, probably related to those found in micellar solutions, do exist in the gas phase. Moreover, modified models derived from the structural analysis of crystals and fibers can be used with a high degree of confidence for bile salt aggregates in the gas phase. In particular, stable aggregates both in the gas phase and in solution are trimers in the case of dihydroxy salts, and dimers in the case of trihydroxy salts. Finally, the evidence from the ESIMS experiments shows that the aggregates of glyco derivatives are more stable than those of tauro derivatives.

Experimental Section

Materials: NaGDC, NaTDC, NaGC, and NaTC (Sigma) were twice crystallized from a mixture of water and acetone. X-ray analysis showed that hexagonal ($P6_5$),[14a] trigonal ($P3_1$),[15b] tetragonal ($I4$),[15d] and monoclinic ($C2$)[12b] crystals of NaGDC, NaTDC, NaGC, and NaTC, respectively, were obtained. All the crystals contained water, and those of NaGC and NaTC also acetone, which was removed from the NaGC and NaTC crystals by heating at 50 °C under a pressure of 10^{-2} Torr before preparation of the aqueous solutions investigated by ESIMS. NaGDC and NaTDC fibers, drawn from concentrated aqueous solutions, were found by X-ray analysis to be preferentially oriented microcrystalline specimens formed by trimers arranged in 7/1 helices.[9a, 12a]

ESIMS measurements: All experiments were performed on a ZABSpec oa TOF mass spectrometer of EBETOF configuration (Micromass Ltd., Manchester, UK), equipped with an electrospray ion source. Aqueous NaGDC, NaTDC, NaGC, and NaTC solutions (1.00×10^{-3} M) were injected and ionized by electrospray at a flow rate of 2 μL min^{-1}. Higher concentrations and flow rates were used when detection of multiply charged aggregates was needed. The electrospray needle was maintained at 4000 V in both the positive- and the negative-ion detection modes. The drying bath gas (N_2) was heated to 80 °C, and its flow rate was adjusted to 5 L min^{-1}. The collisional heating in the interface was controlled by regulating the voltage difference between the nozzle and the skimmer elements (Δ*NS*) in the 0 to +260 V range. The mass spectra were acquired at a mass resolution of 2000 FWHM at *m*/*z* 2000. The charge-state analysis was performed at higher resolution, typically 5000 FWHM at *m*/*z* 2000.

X-ray measurements: X-ray diffraction patterns of NaGC and NaTC crystals were recorded on cylindrical films with a Weissenberg camera. X-ray diffraction patterns of NaGDC and NaTDC fibers were recorded on flat films with a Buerger precession camera. The most intense, accurately known NaCl interplanar spacings were used to determine those of the fibers. Ni-filtered $Cu_{K\alpha}$ radiation ($\lambda = 1.5418$ Å) was used.

Vapor-pressure measurements: The vapor pressures of NaGC and NaTC crystals and of NaGDC and NaTDC fibers were measured by the torsion effusion method,[18] with a previously described apparatus.[19a, b] Conventional graphite torsion cells were used. The instrument calibration constants of the cells were determined by vaporizing pure cadmium, which has well-known vapor-pressure values. Sample temperatures were indirectly measured by a calibrated Pt – Pt*10 % Rh thermocouple inserted in a fixed blank cell placed close below the torsion cell containing the sample. The correct temperature was determined by a standard procedure[19c] that gives an uncertainty not exceeding ±2 K. The uncertainties associated with the instrument constant and the torsion angle measurements produced a displacement in log *P* values of about ±0.08.

Acknowledgements

The financial support of Rome University "La Sapienza", the Ministero dell'Università e della Ricerca Scientifica e Tecnologica (MURST), and the Consiglio Nazionale delle Ricerche (CNR) is gratefully acknowledged. We thank Prof. Vincenzo Piacente for the vapor-pressure measurements.

[1] A. F. Hofmann, D. M. Small, *Annu. Rev. Med.* **1967**, *18*, 333.
[2] D. M. Small in *The Bile Acids*, *Vol. 1* (Eds.: P. P. Nair, D. Kritchevsky), Plenum Press, New York, **1971**, p. 249.
[3] M. C. Carey in *The Liver: Biology and Pathobiology* (Eds.: I. M. Arias, H. Popper, D. Schacter, D. Shafritz), Raven Press, New York, **1982**, p. 429.
[4] M. C. Carey in *Sterols and Bile Acids* (Eds.: H. Danielsson, J. Sjøvall), Elsevier/North-Holland Biomedical Press, Amsterdam, **1985**, p. 345.
[5] D. M. Small, S. A. Penkett, D. Chapman, *Biochim. Biophys. Acta* **1969**, *176*, 178.
[6] a) D. G. Oakenfull, L. R. Fisher, *J. Phys. Chem.* **1977**, *81*, 1838; b) L. R. Fisher, D. G. Oakenfull, *J. Phys. Chem.* **1980**, *84*, 937.
[7] H. Kawamura, Y. Murata, T. Yamaguchi, H. Igimi, M. Tanaka, G. Sugihara, J. P. Kratohvil, *J. Phys. Chem.* **1989**, *93*, 3321.
[8] a) A. Rich, D. M. Blow, *Nature* **1958**, *182*, 423; b) D. M. Blow, A. Rich, *J. Am. Chem. Soc.* **1960**, *82*, 3566.
[9] a) G. Briganti, A. A. D'Archivio, L. Galantini, E. Giglio, *Langmuir* **1996**, *12*, 1180; b) A. A. D'Archivio, L. Galantini, E. Giglio, A. Jover, *Langmuir* **1998**, *14*, 4776; c) A. Bonincontro, A. A. D'Archivio, L. Galantini, E. Giglio, F. Punzo, *J. Phys. Chem. B* **1999**, *103*, 4986; d) E. Bottari, A. A. D'Archivio, M. R. Festa, L. Galantini, E. Giglio, *Langmuir* **1999**, *15*, 2996; e) A. Bonincontro, A. A. D'Archivio, L. Galantini, E. Giglio, F. Punzo, *Langmuir* **2000**, *16*, 10436; f) E. Bottari, M. R. Festa, R. Jasionowska, *J. Inclusion Phenom. Mol. Recognit. Chem.* **1989**, *7*, 443; g) E. Bottari, M. R. Festa, *Monatsh. Chem.* **1993**, *124*, 1119; h) E. Bottari, M. R. Festa, *Langmuir* **1996**, *12*, 1777; i) E. Bottari, M. R. Festa, M. Franco, *Analyst* **1999**, *124*, 887.
[10] G. Esposito, E. Giglio, N. V. Pavel, A. Zanobi, *J. Phys. Chem.* **1987**, *91*, 356.
[11] a) G. Conte, R. Di Blasi, E. Giglio, A. Parretta, N. V. Pavel, *J. Phys. Chem.* **1984**, *88*, 5720; b) G. Esposito, A. Zanobi, E. Giglio, N. V. Pavel, I. D. Campbell, *J. Phys. Chem.* **1987**, *91*, 83; c) E. Chiessi, M. D'Alagni, G. Esposito, E. Giglio, *J. Inclusion Phenom. Mol. Recognit. Chem.* **1991**, *10*, 453; d) M. D'Alagni, M. Delfini, L. Galantini, E. Giglio, *J. Phys. Chem.* **1992**, *96*, 10520.
[12] a) M. D'Alagni, A. A. D'Archivio, E. Giglio, L. Scaramuzza, *J. Phys. Chem.* **1994**, *98*, 343; b) M. D'Alagni, L. Galantini, E. Giglio, E. Gavuzzo, L. Scaramuzza, *Trans. Faraday Soc.* **1994**, *90*, 1523; c) A. A. D'Archivio, L. Galantini, E. Gavuzzo, E. Giglio, L. Scaramuzza, *Langmuir* **1996**, *12*, 4660; d) M. D'Alagni, A. A. D'Archivio, L. Galantini, E. Giglio, *Langmuir* **1997**, *13*, 5811; e) A. A. D'Archivio, L.

  0947-6539/02/0808-1932 $ 20.00+.50/0

Galantini, E. Giglio, *Langmuir* **1997**, *13*, 4197; f) A. A. D'Archivio, L. Galantini, E. Gavuzzo, E. Giglio, F. Mazza, *Langmuir* **1997**, *13*, 3090; g) A. Bonincontro, G. Briganti, A. A. D'Archivio, L. Galantini, E. Giglio, *J. Phys. Chem. B*, **1997**, *101*, 10303.

[13] a) E. Giglio, S. Loreti, N. V. Pavel, *J. Phys. Chem*. **1988**, *92*, 2858; b) E. Burattini, P. D'Angelo, E. Giglio, N. V. Pavel, *J. Phys. Chem*. **1991**, *95*, 7880; c) I. Ascone, P. D'Angelo, N. V. Pavel, *J. Phys. Chem*. **1994**, *98*, 2982; d) P. D'Angelo, A. Di Nola, E. Giglio, M. Mangoni, N. V. Pavel, *J. Phys. Chem*. **1995**, *99*, 5471.

[14] a) A. R. Campanelli, S. Candeloro De Sanctis, E. Chiessi, M. D'Alagni, E. Giglio, L. Scaramuzza, *J. Phys. Chem*. **1989**, *93*, 1536; b) M. D'Alagni, A. A. D'Archivio, E. Giglio, *Biopolymers* **1993**, *33*, 1553.

[15] a) A. R. Campanelli, S. Candeloro De Sanctis, E. Giglio, S. Petriconi, *Acta Crystallogr. Sect. C* **1984**, *40*, 631; b) A. R. Campanelli, S. Candeloro De Sanctis, E. Giglio, L. Scaramuzza, *J. Lipid Res.* **1987**, *28*, 483; c) A. R. Campanelli, S. Candeloro De Sanctis, A. A. D'Archivio, E. Giglio, L. Scaramuzza, *J. Inclusion Phenom. Mol. Recognit. Chem*. **1991**, *11*, 247; d) A. R. Campanelli, S. Candeloro De Sanctis, L. Galantini, E. Giglio, L. Scaramuzza, *J. Inclusion Phenom. Mol. Recognit. Chem*. **1991**, *10*, 367.

[16] E. Bottari, M. R. Festa, M. Franco, *Langmuir* **2002**, in press.

[17] a) D. L. Smith, Z. Zhang, *Mass Spectrom. Rev.* **1994**, *13*, 411; b) R. B. Cole, *J. Mass Spectrom*. **2000**, *35*, 763; c) *Electrospray Ionization Mass Spectrometry* (Ed.: R. B. Cole), Wiley, New York, **1997**, and references therein.

[18] R. D. Freeman in *The Characterization of High Temperature Vapour* (Ed.: J. L. Margrave), Wiley, New York, **1967**.

[19] a) V. Piacente, G. De Maria, *Ric. Sci*. **1969**, *39*, 549; b) M. Adami, D. Ferro, V. Piacente, P. Scardala, *High Temp. Sci*. **1987**, *23*, 173; c) V. Piacente, D. Fontana, P. Scardala, *J. Chem. Eng. Data* **1994**, *39*, 231.

Received: October 1, 2001 [F3582]